JOURNAL OF GEOPHYSICAL RESEARCH: SPACE PHYSICS, VOL. 118, 5317–5326, doi:10.1002/jgra.50470, 2013

Ionization emissions associated with N_2^+ 1N band in halos without visible sprite streamers

C. L. Kuo,[1] E. Williams,[2] J. Bór,[3] Y. H. Lin,[4] L. J. Lee,[4] S. M. Huang,[4] J. K. Chou,[4] A. B. Chen,[4,5] H. T. Su,[4] R. R. Hsu,[4] G. Sátori,[3] H. U. Frey,[6] S. B. Mende,[6] Y. Takahashi,[7] and L. C. Lee [1,8]

Received 17 December 2012; revised 15 June 2013; accepted 22 July 2013; published 20 August 2013.

[1] We report the ionization emission associated with N_2^+ 1N band in a halo event without visible sprite streamers. To avoid the lightning contamination to the ionization emission, we find halos whose parent lightning light is blocked by the Earth's limb. Five halos in the 2004–2010 Imager of Sprites and Upper Atmospheric Lightning data set were identified as halos without visible sprite streamers. A halo with maximum N_2 1P brightness had significant ionization emission of N_2^+ 1N. The time-integrated photon intensity of N_2 1P, N_2 2P, and N_2^+ 1N emission is 2.2×10^5, 2.1×10^4, and 7.4×10^2 photons cm^{-2}, respectively at a distance of 4130 km. The total number of photons of N_2 1P, N_2 2P, and N_2^+ 1N band emissions are 4.6×10^{23}, 4.3×10^{22}, and 1.6×10^{21} photons, respectively. In the halo region, the electron density increased as 1–2 orders of magnitude higher than ambient electron density. From the emission ratio of N_2^+ 1N to N_2 2P, the reduced electric field is estimated to be 275–325 Td that is higher than the conventional breakdown electric field. The recorded electric field related to this halo event is produced by a lightning discharge that has a total charge moment change of −1450 C km. Based on the estimated electric field from optical emissions, it is found that the lightning-induced electric field in the bright halo region is significantly relaxed with a rate faster than that estimated using ambient electron density, in agreement with previous modeling results showing that the electron density enhancement due to the ionization processes leads to a short dielectric relaxation time inside the halo region.

Citation: Kuo, C. L., et al. (2013), Ionization emissions associated with N_2^+ 1N band in halos without visible sprite streamers, *J. Geophys. Res. Space Physics*, *118*, 5317–5326, doi:10.1002/jgra.50470.

1. Introduction

[2] Halos are pancake-like light-emitting objects with diameters of ~80 km, occurring at altitudes of ~80 km [*Barrington-Leigh et al.*, 2001; *Wescott et al.*, 2001; *Miyasato et al.*, 2002; *Bering et al.*, 2004a; *Bering et al.*, 2004b; *Frey et al.*, 2007; *Williams et al.*, 2012]. Halos were initially thought to be elves by most ground observers using conventional cameras with 30 frames per second until *Barrington-Leigh et al.* [2001] first showed that halos are distinct from elves (the latter have a much larger diameter of ~300 km and a shorter luminous duration of ~1 ms). The evolution of halo and elves recorded by a high-speed (3000 frames per second) camera were found to be consistent with the modeling results [*Barrington-Leigh et al.*, 2001]. *Bering et al.* [2002, 2004a, 2004b] checked the optical observations from stratospheric balloons and found halos with negative cloud-to-ground (−CG) lightning. *Frey et al.* [2007] also showed that ~50% of halos are unexpectedly associated with −CG lightning while nearly 99% sprites are induced by positive cloud-to-ground (+CG) lightning. *Wescott et al.* [2001] compared the maximum brightness geometry of halos with lightning locations using triangulation measurements. They found that the maximum brightness of the halo is very close to the location of the parent lightning while the sprite structure can be displaced as far as several tens of kilometers.

[3] It is noticed that the term of "halo/sprite halo" was originally defined by an observed brief diffuse flash at altitudes of ~70−85 km that accompanies or precedes more structured sprites [*Barrington-Leigh et al.*, 2001]. Halos

[1]Institute of Space Science, National Central University, Jhongli, Taiwan.
[2]Parsons Laboratory, Massachusetts Institute of Technology, Cambridge, Massachusetts, USA.
[3]Research Centre for Astronomy and Earth Sciences, GGI, Hungarian Academy of Sciences, Sopron, Hungary.
[4]Department of Physics, National Cheng Kung University, Tainan, Taiwan.
[5]Institute of Space, Astrophysical and Plasma Sciences, National Cheng Kung University, Tainan, Taiwan.
[6]Space Sciences Laboratory, University of California, Berkeley, California, USA.
[7]Department of Cosmosciences, Hokkaido University, Sapporo, Japan.
[8]Institute of Earth Sciences, Academia Sinica, Taipei, Taiwan.

Corresponding author: C. L. Kuo, Institute of Space Science, National Central University, 300 Jhongda Rd., Jhongli 32001, Taiwan. (clkuo@jupiter.ss.ncu.edu.tw)

2169-9380/13/10.1002/jgra.50470

Table 1. Summary of ISUAL Halos Whose Parent Lightning Is Below the Earth's Limb

Trigger Time (UT)	Longitude	Latitude	Average Brightness (kR)[a]	Maximum Brightness (kR)[b]	SP3[c]	N_2^+ 1N[d]	CMC (C km)[e]
11 December 2005 1139:04.777	−168.0	41.6	150	280	No	No	N/A
31 July 2006 0626:29.850	−97.4	15.1	240	720	Yes	Yes	−1450
22 May 2008 0630:47.294	−99.2	7.7	220	640	Yes	No	−750
19 November 2009 11:19:25.962	−175. 9	7.3	150	570	No	No	−880
18 April 2011 2333:43.115	5.9	0.9	130	230	No	No	−920

[a]The average value of brightness recorded by pixels on ISUAL Imager CCD in halo emission region.
[b]The maximum value of brightness recorded by CCD pixels.
[c]Photometric measurement of ISUAL SP3 (centered at 391.4 nm; bandwidth 4.2 nm).
[d]If the contribution of N_2 2P emission is subtracted from photometric measurement of SP3, shown in Figure 3a, the N_2^+ 1N emission is significant with S/N > 3.
[e]The charge moment change (CMC) estimated by the ELF data from the Nagycenk Observatory, Hungary (NCK; 47.62°N, 16.72°E, 513.8 Hz sampling rate, 5–30 Hz passband [*Sátori et al*., 1996; *Sátori and Zieger*, 1996].

and sprite streamers are closely interlinked phenomena, which are both driven by quasi-static electric field produced by lightning. It is possible that sprite streamers do exist in a halo event but they are not observed because they lack the required acceleration and expansion to be bright enough to be detected [*Liu et al*., 2009]. Similarly, only sprite streamers are observed but diffuse halo emissions are too weak to be recognized [*Qin et al*., 2013].

[4] Many authors studied the topics about how a halo developed into sprite streamers [*Pasko et al*., 1996; *Pasko et al*., 1997; *Hiraki and Fukunishi*, 2006; *Luque and Ebert*, 2009; *Hiraki*, 2010; *Qin et al*., 2011, 2012, 2013]. In this paper, we show the analysis of ionization emission associated with N_2^+ 1N (0, 0) in a halo event without visible sprite streamers [*Williams et al*., 2012]. The remotely recorded electric and magnetic field from a ground ELF station for its parent lightning is used to estimate the charge moment change (CMC). We also estimate the magnitude of the electric field from the emission rate ratio of N_2^+ 1N to N_2 2P emission bands in an Imager of Sprites and Upper Atmospheric Lightning (ISUAL) recorded halo. The derived ratio of emission rates shows that the magnitude of the electric field is higher than the conventional breakdown electric field. In this halo event, we also found that significant N_2^+ 1N (0, 0) emission existed in the halo with maximum brightness but without visible steamers.

2. ISUAL Experiment

[5] The ISUAL (Imager of Sprites and Upper Atmospheric Lightning) onboard the FORMOSAT-2 satellite is the first satellite payload dedicated to the survey of Transient Luminous Events (TLEs) [*Chern et al*., 2003; *Kuo et al*., 2005; *Mende et al*., 2005; *Su et al*., 2005; *Chen et al*., 2008; *Kuo et al*., 2008; *Kuo et al*., 2009; *Chang et al*., 2010; *Lee et al*., 2012; *Wu et al*., 2012]. The FORMOSAT-2 is a sun-synchronized satellite with 14 daily-revisiting orbits at an altitude of 891 km. The FORMOSAT-2 was successfully launched on 21 May 2004. The ISUAL experiment is an international collaboration between the National Cheng Kung University, Taiwan, Tohoku University, Japan, and the instrument development team from the University of California, Berkeley. The ISUAL consists of three sensor packages including an intensified Charge-coupled Device (CCD) imager, a six-channel spectrophotometer, and a dual-band array photometer (AP). The imager is equipped with six selectable filters (N_2 1P, 762, 630, 557.7, 427.8 nm filters, and a broadband filter) mounted on a rotatable filter wheel. The spectrophotometer contains six filter photometer channels, their band passes ranging from the far ultraviolet to the near infrared regions. The spectrophotometer (SP) channels include SP1 (150–290 nm), SP2 (centered at 337 nm; bandwidth 5.6 nm), SP3 (centered at 391.4 nm; bandwidth 4.2 nm), SP4 (608.9–753.4 nm), SP5 (centered at 777.4 nm), and SP6 (228.2–410.2 nm). The sampling rate of the ISUAL SP is 10 kHz. The dual-channel AP is fitted with broadband blue and red filters. The mission objectives are to perform a global survey of lightning-induced TLEs, to determine the occurrence rate of TLEs above thunderstorms, to investigate their spatial, temporal, and spectral properties, and to investigate the global distribution of airglow intensity as a function of altitude. ISUAL have completed the first phase (2004–2009) of the orbital mission. Thanks to a successful 5 year mission and significant scientific achievements, additional funding has been granted to the ISUAL team for an extended mission from the National Space Organization in Taiwan.

3. Results and Discussion

3.1. Demonstration of the Existence of N_2^+ 1N (0, 0) Emissions in Halos

[6] We use the photometric measurement with the 391.4 nm filter to identify the emission associated with N_2^+ 1N (0, 0) band. However, ISUAL photometers have a 20 × 5° field of view. The lightning emission at 391.4 nm would also contribute to the photometric measurement for ISUAL recorded halos. The Earth's surface at the limb is a natural blockage for lightning emission. Therefore, we search for halo events without visible sprite streamers whose parent lightning is below the Earth's limb to avoid the lightning contamination for the N_2^+ 1N ionization emission. In 2004 to 2010, ISUAL recorded a large number of halos. But only five halos whose parent lightning originated below the Earth's limb were found in a total of more than 300 halo events in the ISUAL data set. The related parameters associated with those halos are listed in Table 1. Two halo events (31 July 2006 0626:29.850 and 22 May 2008 0630:47.294) have a higher value of brightness than the other three events. We also note that only two of these halos (the same as two mentioned before) with maximum brightness have significant values of ISUAL SP3. If the contribution of N_2 2P emission is subtracted from the photometric measurement of the SP3, shown in Figure 3a,

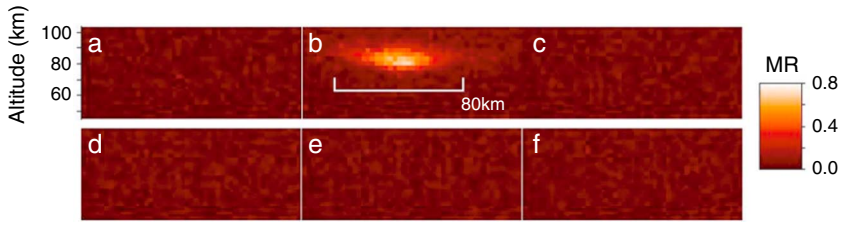

Figure 1. (a–f) The ISUAL recorded image sequences for a halo event at universal time 0626:38.806 on 31 July 2006. The exposure time of each frame is ~30 ms. The halo has a diameter of ~80 km, and its apparent height is at altitudes of ~80–90 km. The average and maximum brightness recorded by the ISUAL Imager is 0.24 and 0.72 Mega Rayleigh (MR).

only the halo (31 July 2006 0626:29.850) with maximum average brightness 240 kR of two mentioned before was verified to have significant N_2^+ 1N emission, which will be discussed later. Although only one of the five halos has definitively identified N_2^+ 1N emission, we cannot reject the possibility the ionization emission exists in other four halo events since we do not know if there were emissions or not; we just know that if there were emissions, they might have been below the detection threshold of photometric measurement (ISUAL SP3), which will be clarified in the end of section 3.1.

[7] Figure 1 shows the ISUAL recorded images for a halo event recorded at UT 0626:38.806 on 31 July 2006. The average and maximum brightness recorded by the ISUAL Imager is 0.24 and 0.72 Mega Rayleigh (MR). Figure 2a shows the observational geometry for the halo event where the distance between the halo and the ISUAL payload onboard FORMOSAT-2 is ~4130 km. The altitudes of the FORMOSAT-2 satellite and halo are 891 km and ~80 km, respectively. The angle between the center of field of view (FOV) and the halo event is 6.5°, shown in Figure 2b. The geometrical center of its parent lightning was located at −97.1°W in longitude and 15.2°N in latitude, shown in Figure 2c.

[8] To trace the ionization emission in the N_2^+ 1N band, we used the ISUAL SP3 photometric reading (centered at 391.4 nm) to retrieve the total N_2^+ 1N band emission. We need to calculate the percentages of halo ionization emissions that fall in the ISUAL SP3. First, we analyze the N_2^+ 1N (0, 0) band spectra and plot the emission bands within the wavelength range of the SP3 response in Figure 3a. The theoretical spectra of the N_2^+ 1N (0, 0) band emission is also overlaid with relative responses of the ISUAL SP3. We multiply the N_2^+ 1N emission intensities with relative responses of ISUAL SP3 and integrate the emission intensities within the wavelength range of the SP3 response. The percentage of N_2^+ 1N emission for the SP3 photometric reading is the ratio of the integrated emission intensity to the total N_2^+ 1N emission band intensity.

[9] Besides N_2^+ 1N (0, 0) emissions, it is found that the pass band of SP3 also includes N_2 2P (3, 6) and N_2 2P (2, 5), shown in Figure 3a. We also need to know the contribution from N_2 2P emissions into the SP3 photometric readings. In Figure 3b, we plot the N_2 2P emission bands overlaid with relative responses of ISUAL SP2. The distribution of the vibrational levels can be described by the Boltzmann temperature $T_{v'}$, where $T_{v'}$ is close to the kinetic temperature of thermal electrons if the vibrational-electronic energy exchange is very efficient. The time scale of the vibrational relaxation for molecular nitrogen at higher temperature ($T_{v'} > 1$ eV) also satisfies the empirical law $p\tau_{v'} \sim 10^{-8}$ atm s [*Millikan and White*, 1963], where p is the gas pressure in units of normal atmospheric pressure (atm) and $\tau_{v'}$ is the vibrational relaxation time in units of seconds. If the vibrational levels can be redistributed, the time scale of the vibrational redistribution must be shorter than the lifetime of the emission band. The typical lifetime of the emission

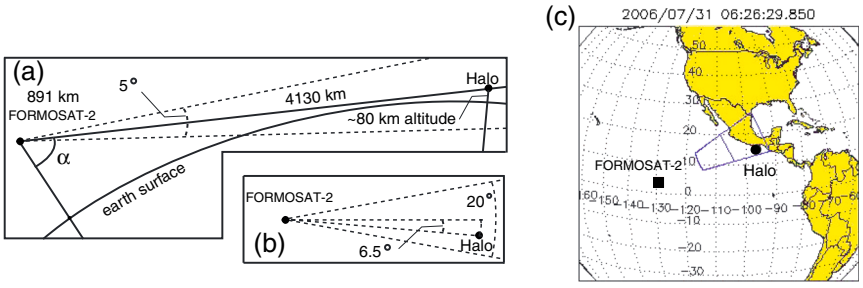

Figure 2. (a) The observational geometry of the halo at UT 0626:38.806 on 31 July 2006. The FOV of the ISUAL Imager and SP is 20° (vertical) × 5° (horizontal). The inclined angle of the halo event with respect to the optical axis of the SP is used to calculate the blue shift of the SP filter response. The nadir angle α between a line of sight of the event and the nadir direction of the FORMOSAT-2 satellite is used to calculate the halo altitude and its mapping latitude and longitude over the Earth's surface. (b) Projected area of the FOV of the Imager and SP. (c) The parent lightning of the halo is located at 97.1°W in longitude and 15.2°N in latitude, shown in filled-circle.

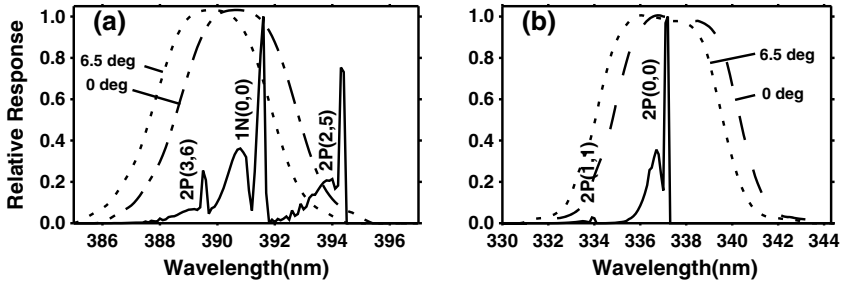

Figure 3. (a) The N_2^+ 1N (0, 0) band of first negative band of N_2^+, N_2 2P (2, 5), and N_2 2P (3, 6) bands of second positive band of N_2, overlaid by the original SP3 (centered at 391.4 nm) response curve and the blue-shifted SP3 response curve (6.5°); (b) N_2 2P (0, 0) and N_2 2P (1, 1) bands of the second positive band of N_2 with SP2 (centered at 337 nm) response curve and blue-shifted SP2 response curve (6.5°).

band is ~50 ns for $2PN_2$. At a halo altitude of ~80 km altitude, $p \sim 10^{-6}$ atm and $\tau_{v'} \sim 10$ ms. The vibrational relaxation time is longer than the lifetime of the $1PN_2$ band. Therefore, our spectra calculation, the distribution of the vibrational levels can be approximated as their Franck-Condon factor $q_{0v'}^{Xu}$ which is a result of direct electron impact. For direct electron impact in discharge phenomena, the pumping density of a specified vibrational level v' of the upper state u is proportional to the Franck-Condon factor. For the relative distribution of the rotational levels in molecular nitrogen, the energy separation between adjacent rotational levels is small in comparison to the translational kinetic energy. The energy exchange rates between transitional and rotational states are high; therefore, the equilibrium temperature of the rotational distribution is very close to the molecular translational temperature, i.e., the ambient temperature. Similarly, the percentages of N_2 2P into SP2 and SP3 photometric readings are calculated, respectively. The same as before, using the SP2 photometric reading and the known percentage of total N_2 2P intensity in the SP2, the total N_2 2P intensity for the halo event can be obtained. Hence, the true N_2 2P intensity in the SP3 photometric reading can be estimated.

[10] We also consider effects from the atmospheric transmittance between the ISUAL SP and the halo event, and the blue shift of filter response due to the angle of incidence. For atmospheric transmittance, we consider the absorption of major atmospheric species, O_2, O_3, and Rayleigh scattering (N_2, O_2). The absorption of N_2 is negligible within the wavelength range of interest. The O_3 density below the 100 km altitude accounts for the majority of O_3 absorption. The details of calculating atmospheric transmittance are found in the work of *Kuo et al*. [2007, 2008]. In section 3.1, the atmospheric transmittance is expressed as a function of the distance between the ISUAL SP and the halo event.

[11] The blueward shift of the center wavelength of the filter response is also considered. The direction of incident emission is not perfectly vertical on the filter plane. The incident light has an inclined angle between the normal vector of the filter plane. The length of a passage of emission light through the SP filter is increased, while the central wavelength of the filter response is also changed. The response waveform of the SP filter at the corresponding wavelength will shift to the blue as the line of sight between SP and the halo event has an incident angle with respect to the optical axis of ISUAL SP. The response of SP2/3 will shift into shorter (blue) wavelength. The formula for the blueward shift effect can be found in *Morrill et al*. [2002] and *Kuo et al*. [2005]. For example, for central wavelength of the filters at 337 and 391.4 nm and the incident light angle, $\theta = 6.5°$, for the halo event, their corresponding wavelength shifts are ~0.7 and ~0.9 nm.

[12] After considering the percentages of band emissions into the SP, the atmospheric transmittances and the blueward shifts of the center wavelength of the filter response, we plot the percentages of band emission (N_2 2P or N_2^+ 1N) into SP2 or SP3 for the halo event with incident light angle $\theta = 6.5°$ as a function of distances. As shown in Figures 4a–4c, at the distance of 4130 km for the halo event, the percentages of N_2 2P into SP2, N_2 2P into SP3, and N_2^+ 1N into SP3 are $21.3 \pm 5\%$, $0.45 \pm 0.04\%$, and $57.8 \pm 5\%$, respectively. The errors of percentages are estimated using the event distance, on average, is less than 50 km for one pixel uncertainty along the line of sight [*Chen et al*., 2008]. We can use the derived percentages to retrieve the total intensities of N_2 2P and N_2^+ 1N from the SP2 and SP3 photometric readings.

[13] The SP-measured photon intensities from N_2 1P, N_2 2P, and N_2^+ 1N in units of 10^6 photons cm^{-2} s^{-1} are shown in Figure 5. It is noted that a significant signal of N_2^+ 1N did exist in the halo emissions with signal-to-noise ratio >3. The peak of the original SP2 and SP3 measurements are 11.4×10^6 and 1.07×10^6 photons cm^{-2} s^{-1}. For the halo event, the percentage of N_2 2P into SP2 is 21.3%, and the total N_2 2P band emission is 11.3×10^6 photons cm^{-2} $s^{-1} \div (21.3 \pm 5)\% = (5.3 \pm 1.2) \times 10^7$ photons cm^{-2} s^{-1}. The contribution of N_2 2P emissions into SP3 measurement is $(5.3 \pm 1.2) \times 10^6 \times (0.45 \pm 0.04)\% = (0.24 \pm 0.06) \times 10^6$ photons cm^{-2} s^{-1}. The SP3 measurement for N_2^+ 1N emission is $1.07 \times 10^6 - (0.24 \pm 0.06) \times 10^6 = (0.83 \pm 0.06) \times 10^6$ photons cm^{-2} s^{-1}. The percentage of N_2 2P into SP2 is 57.8%, and the total N_2^+ 1N emission is $(0.\ 83 \pm 0.06) \times 10^6 \div (57.8 \pm 5)\% = (1.44 \pm 0.16) \times 10^6$ photons cm^{-2} s^{-1}. The ratio of total N_2^+ 1N to N_2 2P emission is $(1.44 \pm 0.16) \times 10^6 \div (5.3 \pm 1.2) \times 10^7 = 0.027 \pm 0.007$ at the time of peak emission in the halo.

[14] Table 2 summarizes the percentages (%) of the major molecular nitrogen bands (N_2 2P, N_2^+ 1N, and N_2 1P) to the channels (SP2, SP3, and SP4) of the ISUAL spectrophotometers. For the distance 4130 km and under the assumption of an isotropic emission source, the total number of time-integrated photons for the specified band emission for the halo event is $4\pi r^2 \times$ (time-integrated photon intensity), where

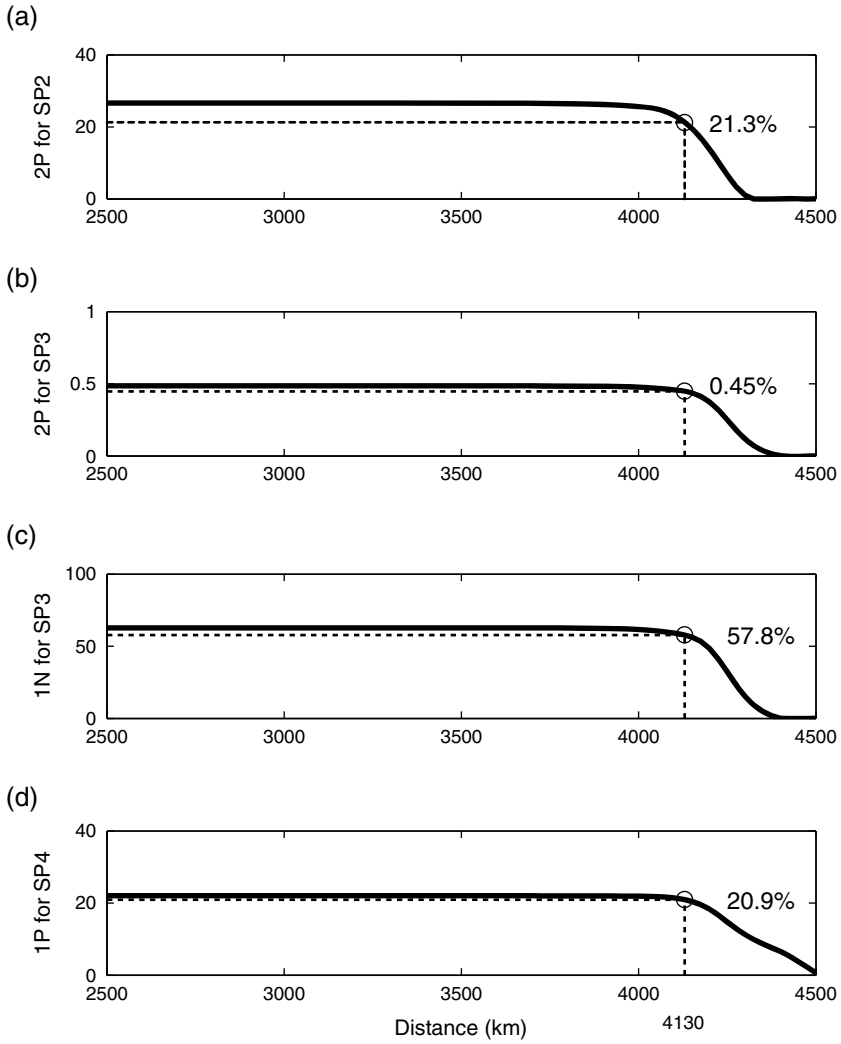

Figure 4. The percentages of (a) N_2 2P for SP2, (b) N_2 2P for SP3, (c) N_2^+ 1N for SP3, and (d) N_2 1P for SP4.

r is the distance 4130 km. The time-integrated photon intensity of N_2 1P, N_2 2P, and N_2^+ 1N emission is 2.2×10^5, 2.1×10^4, and 7.4×10^2 photons cm^{-2}, respectively. For the halo event, the total number of photons of N_2 1P, N_2 2P, and N_2^+ 1N band emission are 4.6×10^{23}, 4.3×10^{22}, and 1.6×10^{21} photons, respectively. The effects of atmospheric transmittance and the blue shift of the SP filter due to the inclined angle of incident light are all considered for our photon calculation.

[15] The detection threshold of photometric measurement (ISUAL SP3) with 391.4 nm filter for N_2^+ 1N (0, 0) emission needs to be addressed. For the halo event (31 July 2006 0626:29.850) with significant N_2^+ 1N emission, the standard deviation of the photometric reading, SP3, is $\sim 0.1 \times 10^6 \div (57.8 \pm 5)\% = (0.17 \pm 0.09) \times 10^6$ photons cm^{-2} s^{-1} for N_2^+ 1N (0, 0) band. For the distance 4130 km and under the assumption of an isotropic emission source, the total number of time-integrated photons for the specified band emission for the halo event is $4\pi r^2 \times$ (time-integrated photon intensity) ~90 photons cm^{-2}. The detection threshold of photometric measurement (ISUAL SP3) has the total number of photons of N_2^+ 1N band, 2×10^{20} photons for the halo event.

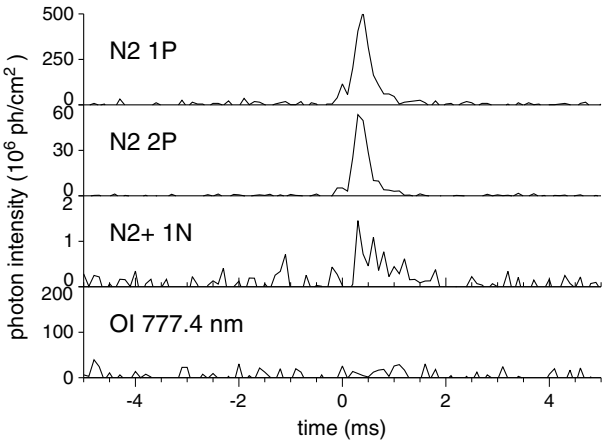

Figure 5. The N_2 1P, 2P, N_2^+ 1N, and O I (777.4 nm) from SP photometric readings for the halo event at UT 0626:38.806 on 31 July 2006. The clear signal for the O I (777.4 nm) channel of SP indicates no lightning contamination. The recorded signals for N_2 1P, 2P, and N_2^+ 1N exist solely from the band emission of halos.

Table 2. The Percentage of N_2 1P, 2P, and N_2^+ 1N Emission Bands in the SP2 (Centered at 337 nm), SP3 (Centered at 391.4 nm), and SP4 (608.9–753.4 nm) Photometric Readings

	SP2	SP3	SP4
N_2 1P	--	--	20.9%
N_2 2P	21.3%	0.45%	--
N_2^+ 1N	0%	57.8%	--

[16] The size of halo is estimated by $\pi r_h^2 d_h \sim 5 \times 10^{19}$ cm^3 where r_h and d_h are 40 km for radius and 10 km for height of the halo. For the halo event (31 July 2006 0626:29.850), the average emission photon density of N_2^+ 1N band is ~32 photons cm^{-3}. The branch ratio of N_2^+ 1N band emission to the total ionizations is 0.093 from the comparisons of peak cross section of ionization of N_2 [*Vallance-Jones*, 1974, p. 104]. The N_2 accounts for ~78.1% of air. The increased electron density in the halo region is estimated to be 32 photons cm^{-3} ÷ 0.093 ÷ 0.781 ~ 440 cm^{-3}. The ambient neutral and electron density is 1.14×10^{14} and 1–10 cm^{-3} at the altitude of 80 km. In halo region, the ionization degree is $\sim 4 \times 10^{-12}$ and the electron density increased as 1–2 orders of magnitude higher than ambient electron density.

3.2. Estimate of the Electric Field in Halos

[17] For the halo event in Figure 1b, the ISUAL Imager shows that the maximum N_2 1P brightness appears in a region near ~80 km altitude, which implies the existence of highly reduced electric field at these altitudes since the maximum halo brightness coincides with the highly reduced electric field. The halo emission rates have a nonlinear relationship with the magnitude of the electric field and increase monotonically with the reduced electric field. At the time of peak emission, at an altitude of ~80 km, the ratio of total N_2^+ 1N to N_2 2P emission derived from the ISUAL SP2 and SP3 measurement is 0.027 ± 0.007 in the previous calculation in section 3.1. The ratio of photometric measured different emission bands is used to estimate the electric field in sprites, which have been used in several studies [*Morrill et al*., 2002; *Kuo et al*., 2005; *Adachi et al*., 2006; *Liu et al*., 2006] and also was recently detailed reviewed by *Pasko* [2010, and references therein]. The electric field measurement using spectral ratios is a very accurate method of spectroscopic diagnostics to estimate the electric field [*Pasko*, 2010].

[18] In this section, we compare the observed ratios of N_2^+ 1N to N_2 2P emissions with the theoretical calculations from ratios of excitation rates of N_2^+ 1N to N_2 2P bands from the (A) *Moss et al*. [2006] and the (B) *Sentman et al*. [2008]. For a more detailed analysis of the temporal evolution of excited bands, we consider the zero-dimensional models: the (C) simple analytic model and the (D) plasma chemistry model [*Sentman et al*., 2008; *Sentman and Stenbaek-Nielsen*, 2009; *Kuo et al*., 2011; *Kuo et al*., 2012] with different applied reduced electric field, E/N, where E is the electric field and N is ambient neutral density. We want to know a reasonable magnitude of the reduced electric field in the halo region for the reported halo event.

[19] Halo emissions are results of time-integrated radiative emissions, which are excited by large-scale ionized waves in the middle atmosphere corresponding to lightning generated electric fields [*Barrington-Leigh et al*., 2001; *Hiraki et al*., 2004; *Hiraki and Fukunishi*, 2006; *Luque and Ebert*, 2009; *Qin et al*., 2011, 2012, 2013]. For the time resolution 0.1 ms of the SP, the ratio of total N_2^+ 1N to N_2 2P emission depends only on the local electric field. The lifetimes of N_2^+ 1N to N_2 2P bands are 70 ns and 50 ns [*Vallance-Jones*, 1974], respectively. Therefore, the difference in time scale of emissions for calculating the emission ratio at the time of peak value is not a serious problem [*Sentman et al*., 2008]. Besides, their projected areas of N_2^+ 1N or N_2 2P emissions also have an impact on the calculated emission ratio since SP integrates all emissions in the FOV of the photometric measurement. We compare the ratio of peak emission of N_2^+ 1N to N_2 2P bands with integration time 0.1 ms for the SP with modeling results, and that would decrease the effect due to the different projected areas of N_2^+ 1N or N_2 2P emissions.

[20] The ambient conductivity at an altitude ~80 km is $\sim 10^{-8}$–10^{-7} S/m, and the corresponding maximum dielectric relaxation time $\tau_\sigma = \varepsilon_0/\sigma$ [*Pasko et al*., 1998] is $8.84 \times 10^{-12}/10^{-8} \sim 1$ ms for conductivity 10^{-8} S/m or 0.1 ms for conductivity 10^{-7} S/m. We used the reduced electric field waveform with different time scale as inputs to excite the N_2 2P and N_2^+ 1N emissions in the optical models. The general waveform of the electric field pulse at a halo altitude 80 km is assumed to be a Gaussian shape,

$$E_v(t) = E_h\left[-(t - t_0)^2/\tau_E^2\right] \quad (1)$$

with peak electric field E_h at time $t_0 = 3\tau_E$ and possible time constants τ_E = 0.01, 0.1, 0.3, 0.5 ms, shown in Figure 6. The choices of τ_E are associated with ambient conductivity, 10^{-8}–10^{-7} S/m or increased conductivity.

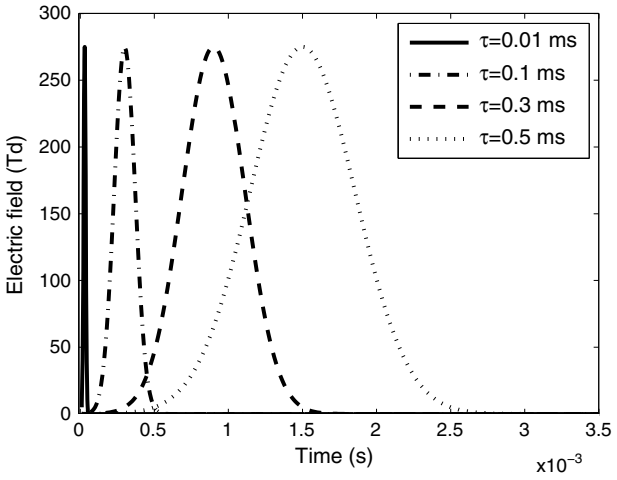

Figure 6. The assumed Gaussian shaped waveform of the electric field pulse in the halo with τ = 0.01, 0.1, 0.3, 0.5 ms to be considered as applied electric fields in our zero-dimensional plasma chemistry models. The derived photon emission rate of the N_2^+ 1N to N_2 2P in comparison with observed ratios is used to estimate the magnitude of the electric field.

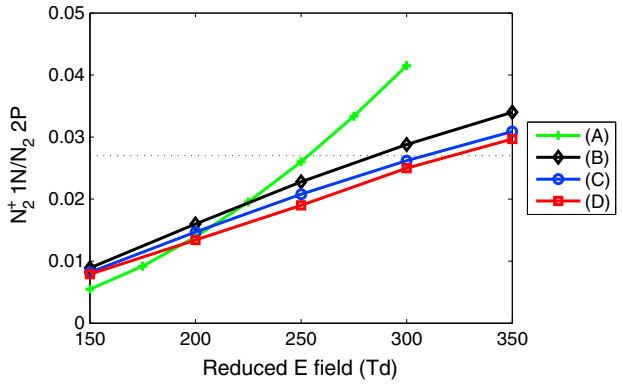

Figure 7. We compare the observed ratios of N_2^+ 1N to N_2 2P emissions with the theoretical calculations from the ratio for the excitation rates of N_2^+ 1N to N_2 2P bands from (A) *Moss et al*. [2006] and (B) *Sentman et al*. [2008]. For a more detailed analysis of the temporal evolution of excited bands, we consider the zero-dimensional models: (C) simple analytic model and (D) plasma chemistry model [*Sentman et al*., 2007; *Kuo et al*., 2011; *Kuo et al*., 2012] with the applied different reduced electric field and find a reasonable magnitude of reduced electric field in the halo region for the reported halo event. The dashed line indicates the value 0.027 derived from the SP photometric readings.

[21] For the (C) simple analytic model, we solve the electron density continuity equation for electric field E_v higher than the conventional breakdown electric field E_k,

$$\frac{dn_e}{dt} = \nu_i n_e, \tag{2}$$

where ν_i is the ionization rate, as a function of electric field E_v (t). The ionization rate coefficients can be checked in the table of *Sentman et al*. [2008]. The analytic solution of electron density in the above equation is written as

$$n_e(t) = n_{e0} e^{\int_0^t \nu_i [E_v(t)] \mathrm{d}t} \tag{3}$$

where the initial electron density n_{e0} is $n_e(t)$ at $t = 0$. We also solve numerically the number density of N_2 ($C^3\prod_u$) and N_2^+ $\left(B^2\Sigma_u^+\right)$, which are upper states of N_2 2P $\left(C^3\prod_u - B^2\Sigma_u^+\right)$ transition and N_2^+ 1N $\left(B^2\Sigma_u^+ - X^2\Sigma_g^+\right)$ transition, respectively. The number density of upper states of N_2 2P and N_2^+ 1N band emissions is provided by

$$\frac{\partial n_k}{\partial t} = \nu_k n_e n_{N_2} - A_k n_k, \tag{4}$$

where n_e and n_{N_2} are the number density of electron and molecular nitrogen; n_{N_2} is 2.8×10^{14} cm^{-3} at halo altitude 80 km; ν_k is a function of the reduced electric field; A_k is the Einstein coefficient, 2.0×10^7 s^{-1} and 1.6×10^7 s^{-1} for N_2 2P and N_2^+ 1N emission bands, respectively.

[22] For the (D) plasma chemistry model at halo altitude of 80 km, we apply the magnitudes of electric field from 150 Td to 350 Td with every step 50 Td to obtain the ratios of N_2^+ 1N to N_2 2P for τ_E = 0.1, 0.3, 0.5 ms. The plasma chemistry model was adopted using the kinetic scheme [*Sentman et al*., 2008; *Kuo et al*., 2011; *Kuo et al*., 2012]. In this scheme, chemical reactions associated with $N_2(C^3\prod_u)$ are initially dominated by the electron-impact process,

$$\mathrm{e} + \mathrm{N_2} \rightarrow e + \mathrm{N_2}\left(C^3\Pi_u\right), \tag{5}$$

and, for longer time scales, $N_2(C^3\prod_u)$ can be excited via the collisional activation reaction with $\mathrm{N_2}\left(\mathrm{A}^3\Sigma_\mathrm{u}^+\right)$ [*Sentman et al*., 2008],

$$\mathrm{N_2}\left(A^3\Sigma_u^+\right) + \mathrm{N_2}\left(A^3\Sigma_u^+\right) \rightarrow \mathrm{N_2}\left(C^3\Pi_u\right). \tag{6}$$

[23] Other chemical reactions associated with number density $N_2(C^3\prod_u)$ are related with the quenching reactions of $N_2(C^3\prod_u)$ with N_2 and O_2,

$$\mathrm{N_2}\left(C^3\Pi_u\right) + O_2 \rightarrow N_2 + O\left(^1S\right) + O\left(^3P\right) \tag{7}$$

and

$$\mathrm{N_2}\left(C^3\Pi_u\right) + N_2 \rightarrow N_2 + N_2\left(a'^1\Sigma_u^-\right). \tag{8}$$

[24] For $N_2^+\left(B^2\Sigma_u^+\right)$, the dominant chemical reaction is the electron-impact process,

$$e + N_2 \rightarrow 2e + N_2^+\left(B^2\Sigma_u^+\right), \tag{9}$$

and the quenching processes with N_2 and O_2 are not important at a halo altitude of 80 km,

$$N_2^+\left(B^2\Sigma_u^+\right) + N_2, O_2 \rightarrow N_2, O_2 + N_2^+\left(X^2\Sigma_g^+\right). \tag{10}$$

[25] The results of the ratio of N_2^+ 1N to N_2 2P emissions from the (D) plasma chemistry model are compared with the (C) simple analytic model at the same magnitude of applied reduced electric field for halo emission ratios.

[26] In Figure 7, the dashed line indicates the measured ratio (~0.027 ± 0.007) from the emission ratio of N_2^+ 1N to N_2 2P in the ISUAL recorded halo, as discussed in section 3.1. The observed ratio is compared with the ratio of photon emission rate from modeling results. We show (A) the ratio of emission rates of N_2^+ 1N to N_2 2P emission in the work of *Moss et al*. [2006], (B) the ratio of emission rates of N_2^+ 1N to N_2 2P in the work of *Sentman et al*. [2008], (C) simple analytic model with τ_E = 0.01, 0.1, 0.3, 0.5 ms, and (D) plasma chemistry model for a time period 0.1, 0.3, and 0.5 ms of the electric field pulse [*Sentman et al*., 2008; *Sentman and Stenbaek-Nielsen*, 2009; *Kuo et al*., 2011; *Kuo et al*., 2012]. In Figure 7, we plot the theoretical calculations from the above models for different time scales of τ_E. The lines for different time scales of τ_E in the model are overlapped in Figure 7.

[27] The photon emission rates of N_2^+ 1N and N_2 2P bands are dominated by their corresponding electron-impact excitation and solely dependent on the magnitude of the peak electric field at time $t = t_0$. Different time scales of τ_E have almost the same values of the emission rate ratios, overlapped in Figure 7. If we consider the complete set of the (D) plasma chemistry model, the results of time periods τ_E = 0.1, 0.3, 0.5 ms of the electric field pulse do not change ratios too much. That implies that photon emission rates of

N_2^+ 1N and N_2 2P bands are mostly dependent on associated electron-impact excitation reactions. Other involved chemical reactions have little effect on the photon emission rates of N_2^+ 1N and N_2 2P bands.

[28] The ratios derived from (A) and (B) are shown in green and black solid lines with data points of "+" and "◇." The results are associated with emission rates of direct electron-impact excitation for N_2^+ 1N to N_2 2P band without considering the electron density. For considering the electron density, the results from (C) and (D) are shown in blue and red solid lines with data points of "" and "□." From equation (3), the electron density is exponentially increased by the time-integrated constant of the ionization rate. The ionization rate is a function of $E_v(t)$, and the time of its maximum value of ionization rate at $t = t_0$ corresponds to the time of maximum electric field from equation (1).

[29] The localized electron density achieves its maximum value at the end of the time period of the applied electric field at a time, $t > t_0 + 3\tau_E$. The emission rate, $\nu_k n_e n_{N_2} A_k$, is proportional to the radiative emission rate (ν_k) of number densities of N_2 ($C^3\Pi_u$) and $N_2^+(B^2\Sigma_u^+)$, which is multiplied by the electron density (n_e), molecular nitrogen density (n_{N_2}), and their Einstein coefficients (A_k). Since the electron density is not reaching its maximum value at the time of maximum electric field, the maximum value of the multiplication will be delayed after the time of electric field, $t = t_0$. Therefore, the time of maximum emission rate is at the time of weaker electric field, following the time of maximum electric field. Therefore, the ratio derived from the (C) simple analytic model has a lower value in comparison with that from (B).

[30] The plasma chemistry model also considers the collisional activation reaction with $N_2(A^3\Sigma_u^+)$ [*Sentman et al.*, 2008] in equation (6). The number density of N_2 $(C^3\Pi_u)$ in the (D) plasma chemistry model has a higher value than that of (C). The increase of emission rate of N_2 2P band will lower the value of the ratio of N_2^+ 1N to N_2 2P, as shown in Figure 7. In Figure 7, the magnitude of the reduced electric field in maximum brightness of halo is implied to be 250 Td in comparison with model (A), or 275–325 Td with models (B), (C), and (D). Recently, modeling studies of halos [*Qin et al.*, 2012, 2013] have shown the case study of +CG with charge moment change 800 C km and the duration of lightning current 0.4 ms. The maximum electric field near the halo altitude 80 km can be as high as ~2 E_k, which is also applicable to the case of −CGs [*Qin et al.*, 2013]. In comparison with the observed halo, the estimated electric field is $2 \sim 3$ E_k where 1 E_k is ~120 Td. If the ambient condition of conductivity and electron density profiles is similar, the estimated CMC of lightning for the observed halo is expected to be higher than 800 C km.

[31] The chemical reactions associated with increased electron density include electron-impact ionization, $e + N_2$, $O_2 \rightarrow N_2^+$, $O_2^+ + 2e$, ionization by heavy particles collision, $N_2(a'^1\Sigma_u^-) + N_2(a'^1\Sigma_u^-) \rightarrow N_2 + N_2 + e$ or $N_2(a'^1\Sigma_u^-) + N_2(A^3\Sigma_u^+) \rightarrow N_2 + N_2 + e$, and charge transfer from associative detachment of N_2 and O_2, $e^- + O_2 \rightarrow O + O^-$ and $O^- + N_2 \rightarrow N_2O + e^-$. From the results of the (D) plasma chemistry model, maximum reaction rate of electron-impact ionization is at least five orders higher than reaction rates of ionization by heavy particle collisions and charge transfer from associative detachment. The increase of electron number density in the halo is dominated by ionization processes with molecular nitrogen and oxygen. We can neglect the contribution from ionization by heavy particles collision and charge transfer from associative detachment of N_2 and O_2. Therefore, the only ionization process in equation (2) is considered in the (C) simple analytic model.

3.3. Impact of the Ionization Processes on the Dielectric Relaxation Time in Halos

[32] We also seek the recorded electric and magnetic field of the parent lightning of halos by a ground station. We cannot estimate the electric field at halo altitudes without considering the relaxation of the electric field since the conductivity at halo altitudes is very high. A lightning discharge can potentially produce an electric field many times higher than the conventional breakdown field at halo altitudes or at higher altitudes. But the electric field cannot penetrate into such high altitudes because of high ambient conductivity. The comparison between the ambient electric field calculated using the total charge moment change and the estimated electric field from halo emissions could only show how fast the field is relaxed by the conductivity in the halo region in order to know if the conductivity is enhanced by the halo. Based on the estimated electric field from the emissions, it is found that the electric field is higher than the conventional breakdown electric field and ionization emission in halo regions is detected. The significant electron density enhancement due to ionization exists in the halo region increases the ambient conductivity. The electric field in the halo region relaxes faster than that expected from the calculation of relaxation time due to ambient electron density, in agreement with previous modeling studies of halos [*Pasko et al.*, 1997; *Qin et al.*, 2011, 2012, 2013].

[33] The Nagycenk Observatory, Hungary (NCK; 47.62°N, 16.72°E, 513.8 Hz sampling rate, 5–30 Hz passband) [*Sátori et al.*, 1996; *Sátori and Zieger*, 1996] provided continuous time series of the vertical electric field and the horizontal magnetic field. They have searched their data archive for ELF transients corresponding to the halos detected by the ISUAL satellite [*Williams et al.*, 2012].

[34] In Table 1, we list the estimated charge moment change (CMC) from NCK ELF data for five halos whose parent lightning originated below the Earth's limb in the ISUAL data set. For the halo (31 July 2006 0626:29.850) with significant N_2^+ 1N emission, NCK ELF data show the parent lightning to be a negative CG flash with an estimated CMC −1450 C km. The halo also had the maximum brightness among the events listed in Table 1. The ISUAL-estimated halo coordinates lie at a ~298° azimuth and a ~10.5 Mm distance from the NCK ELF station where 1 Mm = 10^6 m. The source azimuth and range based in the ELF geolocation are 300° and 11.1 Mm, respectively. The overall distance between the ISUAL-estimated coordinates and the ELF-geolocated coordinates is 680 km, which is quite good for ELF data [*Boccippio et al.*, 1995].

[35] For the halo (31 July 2006 0626:29.850) with significant N_2^+ 1N emission and the estimated CMC −1450 C km. The CMC is expressed by Qh where h is the altitude of the cloud charge and Q is the total charge removed. It is assumed that the altitude of the removed charge for the parent

lightning is ~7 km, and the corresponding removed charge ~200 C. For distances higher than the size of the charge region (several kilometers), the electric field can be simplified as a dipole electric field, the removed charges inside the cloud $\frac{Q}{4\pi\varepsilon_0(z-h)^2}$ and their mirror charges $\frac{-Q}{4\pi\varepsilon_0(z+h)^2}$ for the conductive ground where Q is the removed charge in Coulombs at an altitude h; z is the halo altitude at 80 km; ε_0 is the electric permittivity in free space. For total removed charges 200 C at an altitude of 7 km, the maximum electric field at the halo altitude 80 km is ~100 V/m. The neutral density is 1.14×10^{20} m^{-6} at the altitude of 80 km. The reduced electric field is ~100 V/m/1.14×10^{20} $m^{-6} \sim 8.7 \times 10^{-19}$ V m^2. For 1 Td (Townsend) = 10^{-21} V m^2, the reduced electric field for the recorded charge moment change is ~870 Td, which is much higher than the estimated electric field (275–325 Td) from optical emission ratio. But, as described before, the fast relaxation of the electric field in the halo region should be considered. The estimated electric field using charge moment is three times as great as the estimated electric field from halo emissions, which is overestimated without considering relaxation due to the ambient and increased conductivity at halo altitudes.

[36] The ionization emissions in the observed halo show the evidence of the increased electron density at halo altitudes that also contributes the ambient conductivity. For electric field waveform with Gaussian shape of electric field pulse (250 Td) with $\tau_E = 0.01$, 0.1 ms, as described in equation (3), the electron density is increased as ~1.7 and ~100 times of the ambient electric density. The ambient electron density in the halo region ranges between 10^6 and 10^7 m^{-3}. The increase of electron density also contributes to the conductivity, $\sigma = q_e n_e v_e$, where v_e is the drift velocity with ~10^5–10^6 m/s for magnitude of reduced electric field ~1–3 E_k. The increased ambient conductivity is $q_e n_e v_e \sim 1.6 \times 10^{-19}$ C $\times 10^8$ $m^{-3} \times 10^5$ m/s ~ 10^{-6} S/m. The increased ambient conductivity will shorten the dielectric relaxation time ε_0/σ of electric field to a smaller time period. The increased conductivity 10^{-6} S/m or higher value corresponds to an electric field relaxation time of 0.01 ms or shorter time. The observational evidence discussed in section 3.1 also supports the estimation of conductivity enhancement. For the halo event (31 July 2006 0626:29.850), the electron density increased as 1–2 orders of magnitude higher than ambient electron density. That corresponds to the assumed electric field waveform with Gaussian shape of electric field pulse (250 Td) with $\tau_E \sim 0.01$ ms or shorter time.

[37] The increased ambient electron density will shorten the relaxation time of the electric field and will also lower the peak value of applied electric field by lightning at halo altitudes. For applied electric field E with a shorter relaxation time, the ambient electric field cannot attain its peak value of external electric field E^*. That can be explained by the equation, $\sigma E + \varepsilon_0 \frac{\partial E}{\partial t} = \varepsilon_0 \frac{\partial E^*}{\partial t}$ [*Neubert et al*., 2011]. The above equation satisfies that $\nabla \cdot \nabla \times H = 0$ where H is the magnetic field strength.

[38] Besides the increased conductivity, we discuss another reason to overestimate the electric field at halo altitudes in the previous paragraph. Due to the 5–30 Hz passband of NCK ELF station, the minimum time resolution is ~3.3 ms. Without high time resolution < 1 ms. We cannot obtain the temporal evolution of current moment at the time of halo peak emission. The characteristics of lightning current impulsiveness cannot be resolved. Only the time-integrated current moment is obtained. *Li et al*. [2012] used Duke ULF/ELF sensor (0.1–500 Hz) and resolved the lightning current moment of the parent lightning. Using the Duke ULF/ELF data set, *Lang et al*. [2011] also found the lightning without following sprite still had large CMC, nearly 1400 C km on average. *Lang et al*. [2011, and references therein] suggest that the time variation of the CMC along with parent-lightning current moment may play an important role in determining sprite occurrence. The CMC is not a perfect indicator of sprites productivity. In simulation studies of sprite halo, *Qin et al*. [2013] also concluded a minimum CMC of ~500 C km is required to produce sprites with −CG while only ~350 C km for positive sprites following +CG under typical nighttime conditions. A more impulsive lightning current will produce a brighter halo at halo altitudes and will lead to more intense large-scale ionization. Due to the increased conductivity, the persistence of the electric field is shorter at halo altitudes. That cause of more impulsive ±CG leads to the requirement of a stronger inhomogeneities in order to initiate streamers [*Qin et al*., 2013]. *Williams et al*. [2012] also found the ISUAL recorded halos whose parent lightning −CG with extremely high CMC without identified sprite structure.

[39] In our results, the electric field (250–325 Td) at an altitude 80 km estimated using the ratio of N_2^+ 1N to N_2 2P in the halo region experienced a faster relaxation than that estimated using the ambient electron density, which implies a significant conductivity enhancement due to ionization in the halo region.

4. Summary

[40] To trace ionization emission of the N_2^+ 1N band, we used ISUAL SP2 (centered at 337 nm) and SP3 (centered at 391.4 nm) photometric data to retrieve the N_2^+ 1N ionization emission. The effect of atmospheric transmittance and the blue shift of the SP filter due to the inclined angle of incident light are considered for our photon calculation. For the halo event recorded at UT 0626:38.806 on 31 July 2006, the time-integrated photon intensity of N_2 1P, N_2 2P, and N_2^+ 1N emission is 2.2×10^5, 2.1×10^4, and 7.4×10^2 photons cm^{-2} at the distance of 4130 km. The total photons in the N_2 1P, N_2 2P, and N_2^+ 1N band emission are 4.6×10^{23}, 4.3×10^{22}, and 1.6×10^{21} photons, respectively. The ambient neutral and electron density is 1.14×10^{14} and 1–10 cm^{-6} at the altitude of 80 km. In halo region, the ionization degree is ~4×10^{-12} and the electron density increased as 1–2 orders of magnitude higher than ambient electron density. From the emission ratio of N_2^+ 1N to N_2 2P, the reduced electric field is estimated to be 275–325 Td in comparison with modeling results. The measured electric field in the bright halo region is higher than the conventional breakdown electric field. The recorded electric field related to this halo event is produced by a lightning discharge that has a total charge moment change of −1450 C km. Based on the estimated electric field from optical emissions, it is found that the lightning-induced electric field in the bright halo region is significantly relaxed with a rate faster than that estimated using ambient electron density, in agreement with previous modeling results showing that the electron density enhancement due to the ionization processes leads to a short dielectric relaxation time inside the halo region.

[41] **Acknowledgments.** This work was supported by National Science Council in Taiwan under grants NSC 102-2111-M-008-001 and NSC 101-2628-M-001-007-MY3. We thank F.J. Gordillo-Vázquez and A. Luque for useful discussion. We are also grateful to the National Center for High-Performance Computing in Taiwan and the Center for Computational Geophysics at National Central University for computational supports.

[42] Robert Lysak thanks the reviewers for their assistance in evaluating this paper.

References

Adachi, T., H. Fukunishi, Y. Takahashi, Y. Hiraki, R. R. Hsu, H. T. Su, A. B. Chen, S. B. Mende, H. U. Frey, and L. C. Lee (2006), Electric field transition between the diffuse and streamer regions of sprites estimated from ISUAL/array photometer measurements, *Geophys. Res. Lett.*, *33*, L17803, doi:10.1029/2006GL026495.

Barrington-Leigh, C. P., U. S. Inan, and M. Stanley (2001), Identification of sprites and elves with intensified video and broadband array photometry, *J. Geophys. Res.*, *106*, 1741–1750, doi:10.1029/2000JA000073.

Bering, E. A., III, J. R. Benbrook, J. A. Garrett, A. M. Paredes, E. M. Wescott, D. R. Moudry, D. D. Sentman, H. C. Stenbaek-Nielsen, and W. A. Lyons (2002), Sprite and elve electrodynamics, *Adv. Space Res.*, *30*, 2585–2595, doi:10.1016/S0273-1177(02)80350-7.

Bering, E. A., III, J. R. Benbrook, L. Bhusal, J. A. Garrett, A. M. Paredes, E. M. Wescott, D. R. Moudry, D. D. Sentman, H. C. Stenbaek-Nielsen, and W. A. Lyons (2004a), Observations of transient luminous events (TLEs) associated with negative cloud to ground (−CG) lightning strokes, *Geophys. Res. Lett.*, *31*, L05104, doi:10.1029/2003GL018659.

Bering, E. A., III, L. Bhusal, J. R. Benbrook, J. A. Garrett, A. P. Jackson, E. M. Wescott, D. R. Moudry, D. D. Sentman, H. C. Stenbaek-Nielsen, and W. A. Lyons (2004b), The results from the 1999 sprites balloon campaign, *Adv. Space Res.*, *34*, 1782–1791, doi:10.1016/j.asr.2003.05.043.

Boccippio, D. J., E. Williams, S. J. Heckman, W. A. Lyons, I. Baker, and R. Boldi (1995), Sprites, ELF transients and positive ground strokes, *Science*, *269*, 1088–1091, doi:10.1126/science.269.5227.1088.

Chang, S. C., C. L. Kuo, L. J. Lee, A. B. Chen, H. T. Su, R. R. Hsu, H. U. Frey, S. B. Mende, Y. Takahashi, and L. C. Lee (2010), ISUAL far-ultraviolet events, elves, and lightning current, *J. Geophys. Res.*, *115*, A00E46, doi:10.1029/2009ja014861.

Chen, B., et al. (2008), Global distributions and occurrence rates of transient luminous events, *J. Geophys. Res.*, *113*, A08306, doi:10.1029/2008JA013101.

Chern, J. L., R. R. Hsu, H. T. Su, S. B. Mende, H. Fukunishi, Y. Takahashi, and L. C. Lee (2003), Global survey of upper atmospheric transient luminous events on the ROCSAT-2 satellite, *J. Atmos. Sol. Terr. Phys.*, *65*, 647–659, doi:10.1016/S1364-6826(02)00317-6.

Frey, H. U., et al. (2007), Halos generated by negative cloud-to-ground lightning, *Geophys. Res. Lett.*, *34*, L18801, doi:10.1029/2007gl030908.

Hiraki, Y. (2010), Phase transition theory of sprite halo, *J. Geophys. Res.*, *115*, *A00E20*, doi:10.1029/2009JA014384.

Hiraki, Y., and H. Fukunishi (2006), Theoretical criterion of charge moment change by lightning for initiation of sprites, *J. Geophys. Res.*, *111*, A11305, doi:10.1029/2006JA011729.

Hiraki, Y., L. Tong, H. Fukunishi, K. Nanbu, Y. Kasai, and A. Ichimura (2004), Generation of metastable oxygen atom O(1D) in sprite halos, *Geophys. Res. Lett.*, *31*, L14105, doi:10.1029/2004GL020048.

Kuo, C. L., R. R. Hsu, A. B. Chen, H. T. Su, L. C. Lee, S. B. Mende, H. U. Frey, H. Fukunishi, and Y. Takahashi (2005), Electric fields and electron energies inferred from the ISUAL recorded sprites, *Geophys. Res. Lett.*, *32*, L19103, doi:10.1029/2005GL023389.

Kuo, C. L., et al. (2007), Modeling elves observed by FORMOSAT-2 satellite, *J. Geophys. Res.*, *112*, A11312, doi:10.1029/2007JA012407.

Kuo, C. L., A. B. Chen, J. K. Chou, L. Y. Tsai, R. R. Hsu, H. T. Su, H. U. Frey, S. B. Mende, Y. Takahashi, and L. C. Lee (2008), Radiative emission and energy deposition in transient luminous events, *J. Phys. D.*, *41*, 234014, doi:10.1088/0022-3727/41/23/234014.

Kuo, C. L., et al. (2009), Discharge processes, electric field, and electron energy in ISUAL recorded gigantic jets, *J. Geophys. Res.*, *114*, A04314, doi:10.1029/2008ja013791.

Kuo, C. L., et al. (2011), The 762 nm emissions of sprites, *J. Geophys. Res.*, *116*, A01310, doi:10.1029/2010ja015949.

Kuo, C. L., et al. (2012), Full-kinetic elve model simulations and their comparisons with the ISUAL observed events, *J. Geophys. Res.*, *117*, A07320, doi:10.1029/2012JA017599.

Lang, T. J., J. Li, W. A. Lyons, S. A. Cummer, S. A. Rutledge, and D. R. MacGorman (2011), Transient luminous events above two mesoscale convective systems: Charge moment change analysis, *J. Geophys. Res.*, *116*, A10306, doi:10.1029/2011ja016758.

Lee, L.-J., S.-M. Huang, J.-K. Chou, C.-L. Kuo, A. B. Chen, H.-T. Su, R.-R. Hsu, H. U. Frey, Y. Takahashi, and L.-C. Lee (2012), Characteristics and generation of secondary jets and secondary gigantic jets, *J. Geophys. Res.*, *117*, A06317, doi:10.1029/2011ja017443.

Li, J., S. Cummer, G. Lu, and L. Zigoneanu (2012), Charge moment change and lightning-driven electric fields associated with negative sprites and halos, *J. Geophys. Res.*, *117*, A09310, doi:10.1029/2012ja017731.

Liu, N., et al. (2006), Comparison of results from sprite streamer modeling with spectrophotometric measurements by ISUAL instrument on FORMOSAT-2 satellite, *Geophys. Res. Lett.*, *33*, L01101, doi:10.1029/2005GL024243.

Liu, N. Y., V. P. Pasko, K. Adams, H. C. Stenbaek-Nielsen, and M. G. McHarg (2009), Comparison of acceleration, expansion, and brightness of sprite streamers obtained from modeling and high-speed video observations, *J. Geophys. Res.*, *114*, A00E03, doi:10.1029/2008ja013720.

Luque, A., and U. Ebert (2009), Emergence of sprite streamers from screening-ionization waves in the lower ionosphere, *Nat. Geosci.*, *2*, 757–760, doi:10.1038/ngeo662.

Mende, S. B., H. U. Frey, R. R. Hsu, H. T. Su, A. B. Chen, L. C. Lee, D. D. Sentman, Y. Takahashi, and H. Fukunishi (2005), D region ionization by lightning-induced electromagnetic pulses, *J. Geophys. Res.*, *110*, A11312, doi:10.1029/2005JA011064.

Millikan, R. C., and D. R. White (1963), Systematics of vibrational relaxation, *J. Chem. Phys.*, *39*, 3209–3213.

Miyasato, R., M. J. Taylor, H. Fukunishi, and H. C. Stenbaek-Nielsen (2002), statistical characteristics of sprite halo events using coincident photometric and imaging data, *Geophys. Res. Lett.*, *29*(21), 2033, doi:10.1029/2001GL014480.

Morrill, J., et al. (2002), Electron energy and electric field estimates in sprites derived from ionized and neutral N2 emissions, *Geophys. Res. Lett.*, *29*(10), 1462, doi:10.1029/2001GL014018.

Moss, G. D., V. P. Pasko, N. Liu, and G. Veronis (2006), Monte Carlo model for analysis of thermal runaway electrons in streamer tips in transient luminous events and streamer zones of lightning leaders, *J. Geophys. Res.*, *111*, A02307, doi:10.1029/2005JA011350.

Neubert, T., O. Chanrion, E. Arnone, F. Zanotti, S. Cummer, J. Li, M. Füllekrug, S. Soula, and O. van der Velde (2011), The properties of a gigantic jet reflected in a simultaneous sprite: Observations interpreted by a model, *J. Geophys. Res.*, *116*, A12329, doi:10.1029/2011ja016928.

Pasko, V. P. (2010), Recent advances in theory of transient luminous events, *J. Geophys. Res.*, *115*, *A00E35*, doi:10.1029/2009JA014860.

Pasko, V. P., U. S. Inan, and T. F. Bell (1996), Sprites as luminous columns of ionization produced by quasi-electrostatic thundercloud fields, *Geophys. Res. Lett.*, *23*, 649–652, doi:10.1029/96GL00473.

Pasko, V. P., U. S. Inan, T. F. Bell, and Y. N. Taranenko (1997), Sprites produced by quasi-electrostatic heating and ionization in the lower ionosphere, *J. Geophys. Res.*, *102*, 4529–4562, doi:10.1029/96JA03528.

Pasko, V. P., U. S. Inan, and T. F. Bell (1998), Spatial structure of sprites, *Geophys. Res. Lett.*, *25*, 2123–2126, doi:10.1029/98GL01242.

Qin, J., S. Celestin, and V. P. Pasko (2011), On the inception of streamers from sprite halo events produced by lightning discharges with positive and negative polarity, *J. Geophys. Res.*, *116*, A06305, doi:10.1029/2010JA016366.

Qin, J., S. Celestin, and V. P. Pasko (2012), Formation of single and double-headed streamers in sprite-halo events, *Geophys. Res. Lett.*, *39*, L05810, doi:10.1029/2012GL051088.

Qin, J., S. Celestin, and V. P. Pasko (2013), Dependence of positive and negative sprite morphology on lightning characteristics and upper atmospheric ambient conditions, *J. Geophys. Res. Space Physics*, *118*, 2623–2638, doi:10.1029/2012JA017908.

Sátori, G., and B. Zieger (1996), Spectral characteristics of Schumann resonances observed in Central Europe, *J. Geophys. Res.*, *101*, 29,663–29,670, doi:10.1029/96JD00549.

Sátori, G., J. Szendroi, and J. Vero (1996), Monitoring Schumann resonances--I. Methodology, *J. Atmos. Sol. Terr. Phys.*, *58*, 1475–1481, doi:10.1016/0021-9169(95)00145-X.

Sentman, D. D., and H. C. Stenbaek-Nielsen (2009), Chemical effects of weak electric fields in the trailing columns of sprite streamers, *Plasma Sources Sci. Technol.*, *18*(3), 034012, doi:10.1088/0963-0252/18/3/034012.

Sentman, D. D., H. C. Stenbaek-Nielsen, M. G. McHarg, and J. S. Morrill (2008), Plasma chemistry of sprite streamers, *J. Geophys. Res.*, *113*, D11112, doi:10.1029/2007jd008941.

Su, H., R. Hsu, A. B. Chen, L. Lee, S. B. Mende, H. U. Frey, H. Fukunishi, Y. Takahashi, and C. Kuo (2005), Key results from the first fourteen months of ISUAL experiment, *AGU Fall Meeting Abstracts*, *11*, 01.

Vallance-Jones, A. (1974), *Aurora*, D. Reidel Publishing Co., Dordrecht.

Wescott, E. M., H. C. Stenbaek-Nielsen, D. D. Sentman, M. J. Heavner, D. R. Moudry, and F. T. S. Sabbas (2001), Triangulation of sprites, associated halos and their possible relation to causative lightning and micrometeors, *J. Geophys. Res.*, *106*(A6), 10,467–10,477, doi:10.1029/2000ja000182.

Williams, E., et al. (2012), Resolution of the sprite polarity paradox: The role of halos, *Radio Sci.*, *47*, RS2002, doi:10.1029/2011RS004794.

Wu, Y. J., et al. (2012), Occurrence of elves and lightning during El Niño and La Niña, *Geophys. Res. Lett.*, *39*, L03106, doi:10.1029/2011gl049831.